

# ON THE DESIGN AND USE OF FFT-BASED SPECTRUM ANALYZERS

By

I. KOLLÁR and F. NAGY\*

Department of Measurement and Instrument Technology, Technical University, Budapest

Received June 21, 1981

Presented by Prof. Dr. L. SCHNELL

When designing Fourier analyzers several error sources must be taken into account. In this article after some introductory definitions the errors of the Direct Fourier Transform (DRFT) method are summed up, and then some are treated in detail.

## 1. Groups of signals and spectra

### *Classification of signals*

Figure 1 shows a common classification of signals [1]. The definitions of the enumerated categories:

a) A signal is *deterministic* if and only if it can be represented by explicit mathematical relationships. Any repeated measurement of the source phenomenon results in the same time function.

b)  $x(t)$  is *periodic* if and only if there exists any  $T$  for which  $x(t) \equiv x(t + T)$  for any real  $t$ .

c) At a difference from [1] we define *complex periodic* signals as periodic signals which can be expanded into Fourier series. So the sinusoidal signal is a special case of complex periodic signals.

d)  $x(t)$  is *sinusoidal* if and only if it can be described by the following formula:

$$x(t) = X \sin(2\pi f t + \varphi),$$

where

$X$  = amplitude,

$f$  = frequency,

$\varphi$  = initial phase angle.

e) *Almost periodic* are the signals that are composed of sinusoidal signals, but are not periodic: that is, the ratio of two frequencies in the signal is not rational.

\* Electronic Measuring Gear Works.

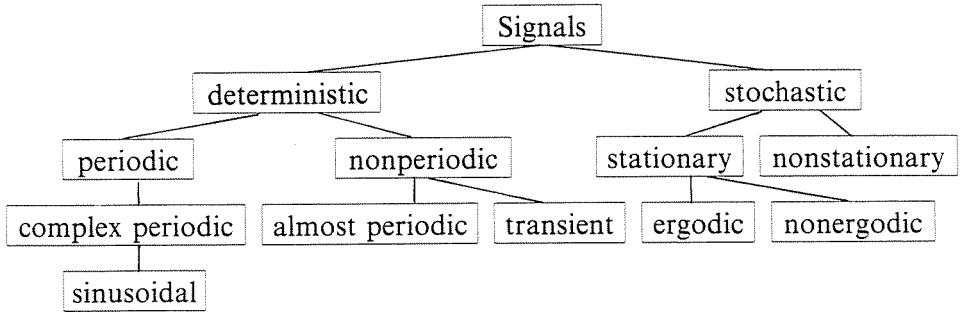


Fig. 1. Classification of signals

f) From the deterministic signals not mentioned yet we define as *transient* the signals that can be Fourier-transformed, that is,

$$\int_{-\infty}^{\infty} |x(t)| dt < \infty .$$

g) *Stochastic* signals are all the signals other than deterministic.

h) Stochastic signals are sample functions of random processes. A random process is *stationary* in the wide sense if and only if the first- and second-order moments and joint moments are time-invariant.

i) Stationary random processes are *ergodic* if and only if ensemble averages (averages over sample functions) do not differ from time averages over a sample function.

For practical reasons sinusoidal, complex periodical and almost periodical signals will be referred to as *sine-type* signals.

### Definitions of energy spectra

a) Energy density spectrum (EDS)

If the time function  $x(t)$  can be Fourier transformed, then by definition,

$$E(f) = \left| \lim_{T \rightarrow \infty} \int_{-\frac{T}{2}}^{\frac{T}{2}} x(t) e^{-j2\pi ft} dt \right|^2 \quad (1)$$

is the EDS of  $x(t)$ . In words,  $E(f)$  is the absolute square value of the Fourier transform of  $x(t)$ . It can be easily shown that

$$\int_{f_0 - \frac{\Delta f}{2}}^{f_0 + \frac{\Delta f}{2}} E(f) df \quad (2)$$

gives the signal's energy carried in the band

$$\left[ f_0 - \frac{\Delta f}{2}, f_0 + \frac{\Delta f}{2} \right].$$

Since the condition of Fourier transforms is

$$\int_{-\infty}^{\infty} |x(t)| dt < \infty,$$

the EDS is only defined for transient signals.

b) Power spectrum (PS)

For signals which can be composed from sine waves:

$$x(t) = \sum_{n=-\infty}^{\infty} c_n e^{j(2\pi f_n t + \varphi_n)},$$

that is, for sine-type signals, the power spectrum is defined as:

$$P(f) = \begin{cases} |c_n|^2 & \text{if } f=f_n, \\ 0 & \text{elsewhere,} \end{cases} \tag{3}$$

where  $P(f)$  denotes the power carried by the signal at frequency  $f$ .

c) Power density spectrum (PDS)

For ergodic stochastic processes the autocorrelation function is defined as:

$$R(\tau) = \lim_{T \rightarrow \infty} \frac{1}{T} \int_{-\frac{T}{2}}^{\frac{T}{2}} x(t)x(t+\tau) dt.$$

The PDS is defined by

$$S(f) = \int_{-\infty}^{\infty} R(\tau)e^{-j2\pi f\tau} dt.$$

It can be shown that

$$\int_{f_0 - \frac{\Delta f}{2}}^{f_0 + \frac{\Delta f}{2}} S(f) df \tag{4}$$

gives the power carried in the band  $\left[ f_0 - \frac{\Delta f}{2}, f_0 + \frac{\Delta f}{2} \right]$ . Defining the Dirac delta operaton  $\delta(t)$  by

$$\int_{-\infty}^{\infty} y(t)\delta(t) dt = y(0),$$

and dealing with  $\delta(t)$  as a “function” (though in the strict sense it is not), it can be shown that for sine-type signals

$$S(f) = \sum_{-\infty}^{\infty} |c_n|^2 \delta(f - f_n) \quad (5)$$

has the same practical meaning as for stochastic signals. Notice that (5) differs from (3) only in the Dirac delta multipliers.

It can be proven [1] that there exists another way to compute  $S(f)$ :

$$S(f) = E \left\{ \lim_{T \rightarrow \infty} \frac{1}{T} \left| \int_{-\frac{T}{2}}^{\frac{T}{2}} x(t) e^{-j2\pi f t} dt \right|^2 \right\} \quad (6)$$

for stochastic and sine-type signals as well.

The expression

$$\frac{1}{T} \left| \int_{-\frac{T}{2}}^{\frac{T}{2}} x(t) e^{-j2\pi f t} dt \right|^2$$

is often called periodogram.

## 2. Measuring principles of spectra

On the basis of the above expressions there are several ways to obtain spectra. They can be classified into three main groups.

a) Use of bandpass filters

On the basis of (2) and (4), let the signal pass through bandpass filters and measure the power (energy) on their outputs. This principle is used e.g. in the heterodyne spectrum analyzers.

b) Computing  $R(\tau)$

For sine-type and stochastic signals an estimate  $R(\tau)$  can be computed and this can be used to obtain the spectrum estimate:

— Performing FFT, a well established method.

— Using identification methods to estimate parameters of a linear stochastic process model; this technique gives generally a better resolution than the former one, but:

— needs a big computing capacity;

— needs some a priori knowledge of the spectrum;

— the methodology is still deficient.

c) Based on DRFT

Taking the finite Fourier transform of  $x(t)$  and then the absolute value of its 2nd power, the energy spectra can be achieved, disregarding multipliers (see (1) and (6)).

The speed of FFT techniques provides superiority over direct  $R(\tau)$  estimation; at lower frequencies the increased stability of digital signal processing, the higher resolution and use of total information provide superiority over the bandpass filter method. That is why our attention is focused on the Direct Fourier Transform (DRFT) method.

### 3. Errors introduced by DRFT

DRFT introduces deterministic and stochastic errors, that are summarized in this chapter.

#### a) Sampling

Sampling means the transformation of the continuous-wave signal to a finite duration pulse train (Fig. 2). Due to the Nyquist sampling theorem, the sampling frequency has to be at least twice as high as the highest frequency present in the analyzed signal:

$$f_s = \frac{1}{\Delta t} > 2B.$$

In order to avoid aliasing a lowpass filter must be used before sampling; this filtering *limits* the signal *frequency* to  $\left(\frac{f_s}{2} = \frac{1}{2\Delta t}\right)$ . The truncation in time domain can be modelled by multiplying by a so-called *time window*. This multiplication means convolution in the frequency domain: the *resolution worsens*, and because of lags, farther points of the exact spectrum influence the actual value of the transformed function. This phenomenon is called *leakage*.

When analysing a sine wave,  $S(f)$  should consist of two Dirac  $\delta$ -s. The convolution with the window function means that  $\hat{S}(f)$  consists of two, appropriately positioned window functions (Fig. 4). Now, using DRFT yields

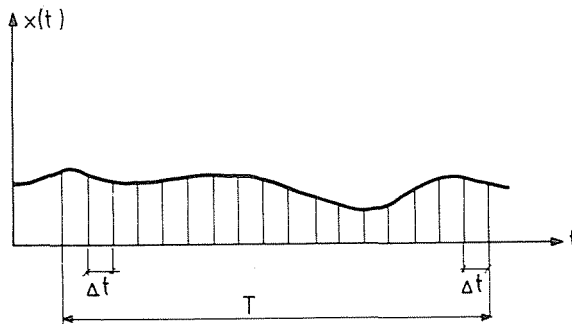


Fig. 2. Sampling

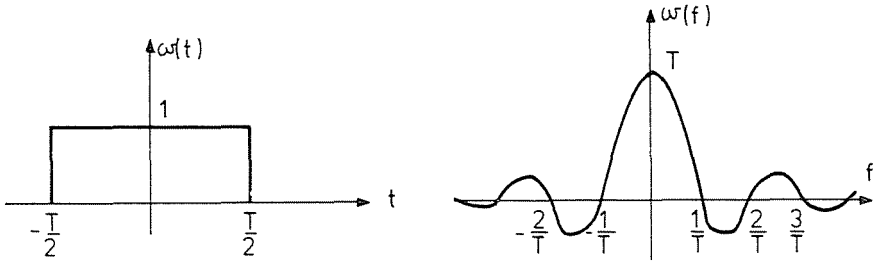


Fig. 3. The rectangular window function

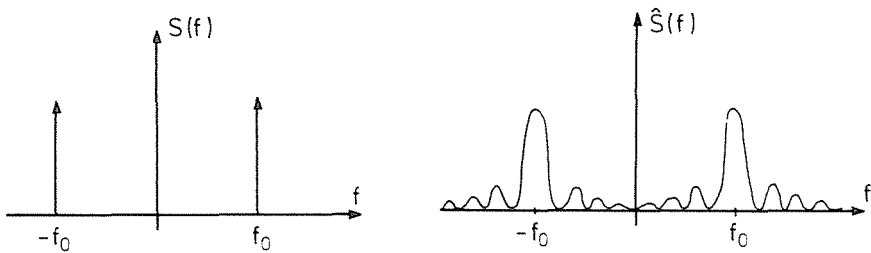


Fig. 4. DRFT spectral estimation of a sine wave

spectrum points in the  $\frac{k}{T}$  positions alone. So if  $\frac{k}{T} \neq f_0$ , the maximum  $\hat{S}(f)$  value is not equal to  $\frac{|c_n|^2}{\Delta f}$  (Fig. 5). Thus, the spectra-based sine amplitude measurement is distorted if  $\frac{k}{T} \neq f_0$ . Plotting this distortion as a function of the sine frequency  $f_0$ , the diagram of Fig. 6 can be obtained. This effect is called *picket fence effect* and depends on the window shape. All effects of truncation can be modified by modifying the truncating function (window function).

## b) Quantization

In order to be manageable for a digital processor, each sampled value is transformed to a finite-bit number. This nonlinear operation is difficult to investigate indeed; some recent work has been reported in [2]. If the quantum size is small enough in comparison with the signal amplitude (e.g. 10%), the effect of quantization can be well modelled by an additive, uniform amplitude distribution white noise (Fig. 7). The distortion of second-order moments (e.g. spectra) affected by *quantization* can be eliminated by the so-called dither-technique (Fig. 8).

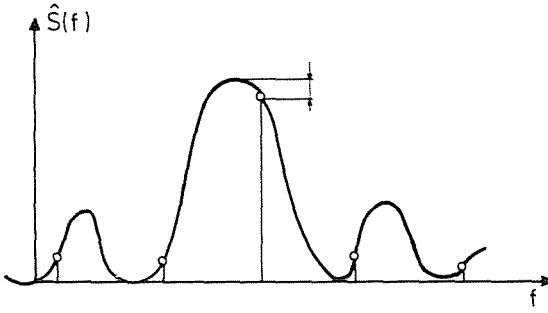


Fig. 5

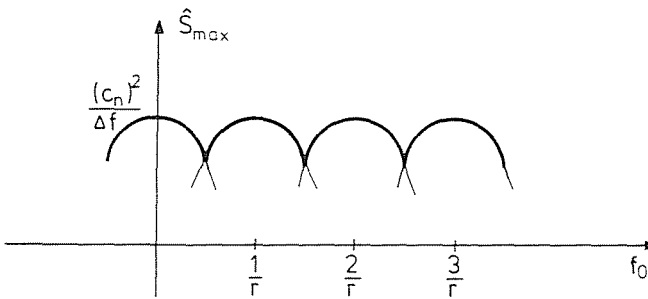


Fig. 6. The picket fence effect

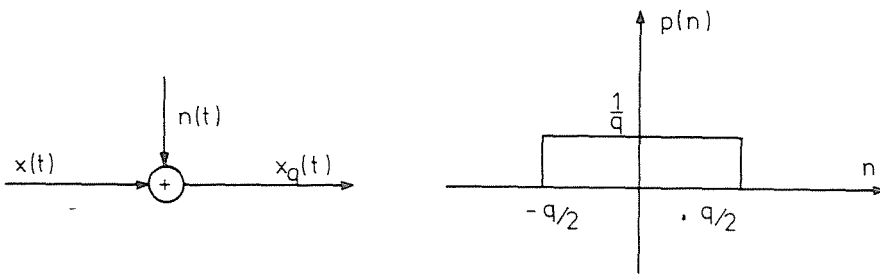


Fig. 7. The model of quantization noise

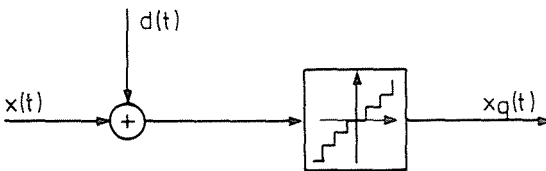


Fig. 8. The dithering technique

If  $d(t)$  is a uniform distribution independent white noise between  $\left[-\frac{d}{2}, \frac{d}{2}\right]$ , ( $d = k \cdot q$  where  $q$  denotes the quantum size, and  $k$  is a positive integer), then there will be no distortion due to quantization, only an additive constant should be removed. Instead of the uniform distribution, noise signals of other distributions may be chosen, which are easier to produce (Gaussian, sinusoidal), with a standard deviation  $\sigma > q$ , but these dithers only reduce and do not eliminate the distortion.

### c) DFT

The FFT algorithm causes *roundoff errors*. This has two sources:

— the complex coefficients are represented in words of finite length: that is, they are quantized:

— performing additions and multiplications the partial results are rounded.

Roundoff errors can be modelled by means of an additive white noise.

The speed of analysis is determined by the speed of the FFT processor so that this can be a bottleneck in the system.

When measuring stochastic signals another problem arises as well. It is well-known that the relative variance of the periodogram is approximately 100% [1]. Thus, results have to be averaged in order to reduce variance; this naturally means a longer analysis time.

Finally, let us briefly consider the problem of resolution. The DFT gives points in the  $\frac{k}{T}$  points of the frequency axis. That is, the absolute resolution is

limited by DFT to  $\frac{1}{T}$ . Thus the relative resolution is smaller at lower frequencies and greater at higher frequencies. These facts may often be disadvantageous. Let us mention here that the relative resolution can be equalized by frequency warping [3], and the absolute resolution can be increased by band-selectable Fourier analysis [4] or Zoom FFT [5].

Let us sum up the DRFT errors:

1. Inexact timing at sampling and non-ideal sampling;
2. Limited upper frequency due to sampling;
3. Limited dynamics due to truncation (limited record length);
4. Leakage (because of limited record length);
5. Picket fence effect (because of limited record length in the case of sine-type signals);
6. Quantization distortion;
7. Distortion due to nonlinear overall characteristics of the quantizer;



8. Increased variance due to quantization;
9. Roundoff errors (distortion, variance);
10. Limited transform speed;
11. 100% relative variance when measuring stochastic signals;
12. Resolution limited to  $\frac{1}{T} = \frac{f_s}{N}$ ;
13. Non-uniform relative resolution (uniform absolute resolution).

It is obvious that reduction of certain errors may give rise to others. For instance, dithering reduces quantization errors, but increases variance. Greater  $N$  increases resolution but increases roundoff variance and transform time as well. So when designing spectrum analyzers the development engineer has to carefully choose a reasonable compromise between contradictory demands. The aim of the following chapters is to give general expressions and design formulas for some of the DRFT errors.

#### 4. Approximate computation of variance caused by quantization

In this chapter we intend to use the model illustrated in Fig. 7. The quantization effect is modelled by an additive white noise uniform distribution on  $\left[-\frac{q}{2}, \frac{q}{2}\right]$ . Thus,

$$E\{n\} = 0, \quad \text{Var}\{n\} = \frac{q^2}{12}.$$

Since the signal  $n(t)$  can be considered as a realization of a random process, its PDS estimator can be computed:

$$\hat{S}_n(f, T) = \frac{1}{T} |\mathcal{F}_T\{n(t)\}|^2.$$

Let  $\mathcal{C}_T$  and  $\mathcal{S}_T$  denote the finite cosine and sine transforms respectively:

$$\mathcal{C}_T\{n(t)\} = \int_{-\frac{T}{2}}^{\frac{T}{2}} n(t) \cos(2\pi ft) dt,$$

$$\mathcal{S}_T\{n(t)\} = \int_{-\frac{T}{2}}^{\frac{T}{2}} n(t) \sin(2\pi ft) dt.$$

So

$$\hat{S}_n(f, T) = \frac{1}{T} |\mathcal{C}_T\{n(t)\} - j\mathcal{S}_T\{n(t)\}|^2 = \frac{1}{T} |\eta_1 - j\eta_2|^2 \quad (7)$$

Since their expressions contain integration, and  $n(t)$  is a white noise,  $\eta_1$  and  $\eta_2$  are normally distributed random variables. For any  $f = \frac{k}{T}$ , provided  $k \neq 0$ , it is easy to show that  $\eta_1$  and  $\eta_2$  are independent, their mean is zero and their variance is equal, that is,  $T \cdot S_n(f, T)/2$  (see(7)). Thus,  $\hat{S}_n(f, T)$  is of  $\chi^2_2$  distribution:

$$E\{\hat{S}_n(f, T)\} = S_n(f, T),$$

$$\text{Var}\{\hat{S}_n(f, T)\} = S_n^2(f, T).$$

Now for the discrete DRFT with parameters

$$N \cdot \Delta t = T$$

the expression of  $S_n(f, T)$  will be derived. Since  $n(t)$  is a white noise,  $S_n(f, T)$  is constant, consequently

$$\frac{q^2}{12} = R_n(0) = \int_{-\frac{f_s}{2}}^{\frac{f_s}{2}} S_n(f, T) df = f_s \cdot S_n(f, T) = \frac{N}{T} \cdot S_n(f, T).$$

So

$$S_n(f, T) = \frac{q^2 T}{12N}.$$

The variance is approximately  $S_n^2(f, T)$  in the discrete case as well, since  $\eta_1$  and  $\eta_2$  are approximately normally distributed.

Let us introduce now the following notations:

$$\check{\zeta}_1 = \mathcal{C}_T\{x(t)\}, \quad \check{\zeta}_2 = \mathcal{S}_T\{x(t)\},$$

and examine the EDS and PDS estimators.

### Energy density spectrum estimator

$$\begin{aligned} \hat{E}_{xq}(f, T) &= |\mathcal{F}_T \{x(t) + n(t)\}|^2 = |\zeta_1 - j\zeta_2 + \eta_1 - j\eta_2|^2 = \\ &= \underbrace{\zeta_1^2 + \zeta_2^2}_{\hat{E}_x(f, T)} + \underbrace{\eta_1^2 + \eta_2^2}_{T \cdot \hat{S}_n(f, T)} + 2\zeta_1\eta_1 + 2\zeta_2\eta_2. \end{aligned}$$

Here  $x(t)$  is deterministic, so

$$E\{\hat{E}_{xq}(f, T)\} = E_x(f, T) + \frac{q^2 T^2}{12N},$$

$$\text{Var}\{\hat{E}_{xq}(f, T)\} = \left(\frac{q^2 T^2}{12N}\right)^2 + 2E_x(f, T) \frac{q^2 T^2}{12N}.$$

### Power density spectrum estimator

Let us decompose  $x(t)$  into two components:

$$x(t) = x_d(t) + x_s(t),$$

where  $d$  denotes the deterministic (periodic) part, and  $s$  denotes the stochastic part.

$$\mathcal{F}_T \{x(t)\} = \zeta_{1d} - j\zeta_{2d} + \zeta_{1s} - j\zeta_{2s}$$

For the stochastic part similar expressions can be derived as for  $n(t)$ .  $\zeta_{1s}$  and  $\zeta_{2s}$  are approximately normally distributed with zero mean and  $T \cdot S_{xs}(f, T)/2$  variance, provided that  $f = \frac{k}{T}$ ,  $k \neq 0$ . So the mean and variance of  $\hat{S}_{xq}(f, T)$ :

$$E\{\hat{S}_{xq}(f, T)\} = S_x(f, T) + \frac{q^2 T}{12N},$$

$$\text{Var}\{\hat{S}_{xq}(f, T)\} = \left[S_{xs}(f, T) + \frac{q^2 T}{12N}\right]^2 + 2S_{xd}(f, T) \left[S_{xs}(f, T) + \frac{q^2 T}{12N}\right].$$

The relative variance is:

$$\begin{aligned} \varepsilon_r^2 \{ \hat{S}_{xq}(f, T) \} &= \left[ \frac{S_{xs}(f, T)}{S_x(f, T)} + \frac{q^2 T}{12NS_x(f, T)} \right]^2 + \\ &+ 2 \frac{S_{xd}(f, T)}{S_x(f, T)} \left[ \frac{S_{xs}(f, T)}{S_x(f, T)} + \frac{q^2 T}{12NS_x(f, T)} \right]. \end{aligned}$$

With the shorthand

$$K = \frac{S_{xs}(f, T)}{S_x(f, T)},$$

$$\begin{aligned} \varepsilon_r^2 \{ \hat{S}_{xq}(f, T) \} &= \left[ K + \frac{q^2 T}{12NS_x(f, T)} \right]^2 + \\ &+ 2(1-K) \left[ K + \frac{q^2 T}{12NS_x(f, T)} \right]. \end{aligned}$$

There are cases when we are interested only in the deterministic part:

$$K_d = \frac{S_{xs}(f, T)}{S_{xd}(f, T)}$$

$$\begin{aligned} \varepsilon_{rd}^2 \{ \hat{S}_{xq}(f, T) \} &= \left[ K_d + \frac{q^2 T}{12NS_{xd}(f, T)} \right]^2 + \\ &+ 2 \left[ K_d + \frac{q^2 T}{12NS_{xd}(f, T)} \right]. \end{aligned} \quad (8)$$

### Discussion

From the above results it can be concluded that the mean of the estimator is changed by an additive constant which can be removed without difficulty; the variance is increased as well, but it depends on the signal to be analyzed. The variance can be reduced by reducing  $T$ . The variance can be approximated in

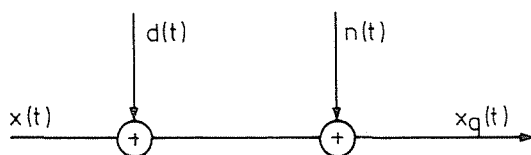


Fig. 9. The noise model of dithering

extreme cases: if

$$\frac{q^2 T}{12 N S_x(f, T)} \ll 1$$

$$\varepsilon_r^2 \{ \hat{S}_{xq}(f, T) \} \begin{cases} \frac{2 T}{6 N S_x(f, T)}, & K \approx 0 \\ 1 + \frac{q^2 T}{6 N S_x(f, T)}, & K \approx 1 \end{cases}$$

The above results can be generalized for the case of dithering as well. If the signal is not approximately constant (e.g. the amplitude could be too small), the quantization noise and the dither are approximately independent, and a white noise model can be used with zero mean and variance

$$\frac{q^2 + d^2}{12}$$

In this case substituting  $(q^2 + d^2)$  for  $q^2$  yields the correct results.

Finally we should like to point out an important circumstance: all the derivations consider the case of a one-channel analyzer. For the case of cross Fourier analyzers with dependent or independent dithers similar results can be obtained.

### A numerical example

A sine wave covered by noise is to be detected by spectral analysis. Let the variance of the noise be  $\sigma^2$ , the amplitude of the sine wave  $U_p > \frac{\sigma}{3}$ , and the frequency  $f_0$ . An FFT processor with an  $N = 2^{10}$  point FFT can be used. Let us compute the maximum value of  $q$  with which the existence of the sine wave can still be detected without averaging (not taking into account the other sources of variance).

Solution:

The relationships for the sine wave and for the noise are:

$$S_{xd}(f_0) = \frac{U_p^2}{4\Delta f} = \frac{U_p^2}{4} \cdot T$$

and

$$S_{xs}(f) = \sigma^2 \cdot \Delta t,$$

respectively. The signal is detected if the  $S/N$  ratio with respect to  $S_{xd}(f, T)$  at  $f_0$  is at least 3:1, i.e.

$$\varepsilon_{rd}^2 < \frac{1}{9}.$$

From (8):

$$K_d = \frac{4\sigma^2}{U_p^2 N},$$

$$\varepsilon_{rd}^2 = \left[ \frac{4\sigma^2}{U_p^2 N} + \frac{q^2 T}{12N \frac{U_p^2}{4} T} \right]^2 + 2 \left[ \frac{4\sigma^2}{U_p^2 N} + \frac{q^2 T}{12N \frac{U_p^2}{4} T} \right].$$

Using  $U_p > \frac{\sigma}{3}$  the following inequalities can be obtained:

$$\varepsilon_{rd}^2 < \left[ \frac{36}{N} \left( 1 + \frac{1}{12} \frac{q^2}{\sigma^2} \right) \right]^2 + 2 \left[ \frac{36}{N} \left( 1 + \frac{1}{12} \frac{q^2}{\sigma^2} \right) \right] < \frac{1}{9},$$

$$q < 2.5\sigma.$$

This means that a rather rough quantizer can fulfil the requirements.

### 5. The analysis of Welch's method for the variance reduction in the estimation of Power Density Spectra

To reduce biasing and variance of the periodogram Welch suggested a new method [6] based on averaging over modified periodograms. The modified periodogram is defined in the continuous case as follows:

$$I_x(f, \tau) = \frac{1}{T_e} |X'(f, \tau)|^2, \quad (9)$$

where

$$X'(f, \tau) = \mathcal{F}\{x(t + \tau) \cdot w(t)\} = \int_{-\infty}^{\infty} x(t + \tau)w(t)e^{-j2\pi ft} dt,$$

and

$$T_e = \int_{-\infty}^{\infty} w^2(t) dt = \int_{-\infty}^{\infty} W^2(f) df.$$

$w(t)$  is called data or time window. It is a real, even and Fourier transformable function, with support<sup>1</sup>  $\left[-\frac{T}{2}, \frac{T}{2}\right]$ . The Fourier-transform of the time window is called spectral window:

$$\mathcal{F}\{w(t)\} = W(f) \tag{10}$$

The sum of periodograms belonging to different segments is Welch's estimator:

$$\hat{S}_x(f) = \frac{1}{K} \sum_{i=0}^{K-1} I_x(f, i \cdot \Delta\tau) \tag{11}$$

*Expected value of the estimator*

It is well-known that the periodogram is a biased estimator [1] with an expected value:

$$E\{\hat{S}_x(f)\} = \frac{1}{T_e} \int_{-\infty}^{\infty} S_x(f - \nu)W^2(\nu) d\nu = \frac{1}{T_e} \mathcal{F}\{R_x(\tau)(w*w)_\tau\}, \tag{12}$$

where  $*$  denotes the convolutional integral.

So the expression for the bias is:

$$E\{S_x(f) - \hat{S}_x(f)\} = \frac{1}{T_e} \int_{-\infty}^{\infty} R_x(\tau) [1 - (w*w)_\tau] e^{-j2\pi f\tau} d\tau. \tag{13}$$

Its upper limit:

$$|E\{S_x(f) - \hat{S}_x(f)\}| \leq \frac{1}{T_e} \int_{-\infty}^{\infty} |R_x(\tau) [1 - (w*w)_\tau]| d\tau. \tag{14}$$

<sup>1</sup> The support  $\left[-\frac{T}{2}, \frac{T}{2}\right]$  means that the function is equal to zero outside the interval.

Random processes have continuous spectra, and their covariance functions are generally absolute integrable, so the biasing may be whatever small, if the support of  $w(\tau)$  is large enough. For this reason, in the stochastic case it is not crucial how to choose a window.

It is a different problem to estimate spectra of sine-type signals. There are two effects which make necessary to deal with the window problem: the spectral leakage and the picket-fence effect or amplitude uncertainty. The spectral leakage can be reduced by reducing the sidelobes of the window, and the amplitude uncertainty by reducing the ripple in the frequency interval

$$\left[ -\frac{1}{2T}, \frac{1}{2T} \right].$$

HARRIS and NUTTALL formed some optimum windows [7, 9] for minimum sidelobes. These windows have the form of

$$w(t) = \text{rect}\left(\frac{t}{T}\right) \sum_{k=-M}^M C_k e^{+j\frac{2\pi}{T}kt} \quad (15)$$

in time domain, and

$$W(f) = T \cdot \sum_{k=-M}^M C_k \text{sinc}(fT - k) \quad (16)$$

in frequency domain, where

$$C_{-k} = C_k \quad \text{for all } k - s$$

$$\text{rect}(x) = \begin{cases} 1 & \text{if } |x| \leq \frac{1}{2}, \\ 0 & \text{elsewhere;} \end{cases}$$

$$\text{sinc}(x) = \mathcal{F}\{\text{rect}(x)\} = \begin{cases} \frac{\sin \pi x}{\pi x} & \text{if } x \neq 0, \\ 1 & \text{if } x = 0. \end{cases}$$

HARRIS minimized the maximum sidelobe for  $M=2$  and  $M=3$ , but did not mind the large amplitude uncertainty.

In the low frequency spectrum analyzer HP 3582 a so-called flat-top window with a wide dynamic range (90.5 dB) and little amplitude uncertainty (0.1 dB) was used [8]. We developed a new window for spectral estimation of sine-type signals. It has as good figures of merit as the flat-top window. The course of development was the following:



Writing  $W(f)$  in the form of (16), then

$$W'(f) = \sum_i W(f - i/T) a_i \quad (17)$$

has the same form, but  $M$  increases depending on the number of summations. This operation makes the window wider, so the picket-fence effect decreases, and so does the dynamic range. Choosing the 4-sample Blackman-Harris window ( $M=3$ ) [7] as a basis and summing three windows, one per cent ripple of  $W'(f)$  has been achieved in the frequency range

$$\left[ -\frac{1}{2T}, \frac{1}{2T} \right].$$

For improving the dynamic range of the obtained window the coefficients were modified by iteration with the aid of the gradient search technique.

The window coefficients are:

$$C_0 = 1$$

$$C_1 = 0.93899$$

$$C_2 = 0.60638$$

$$C_3 = 0.18329$$

$$C_4 = 0.01554$$

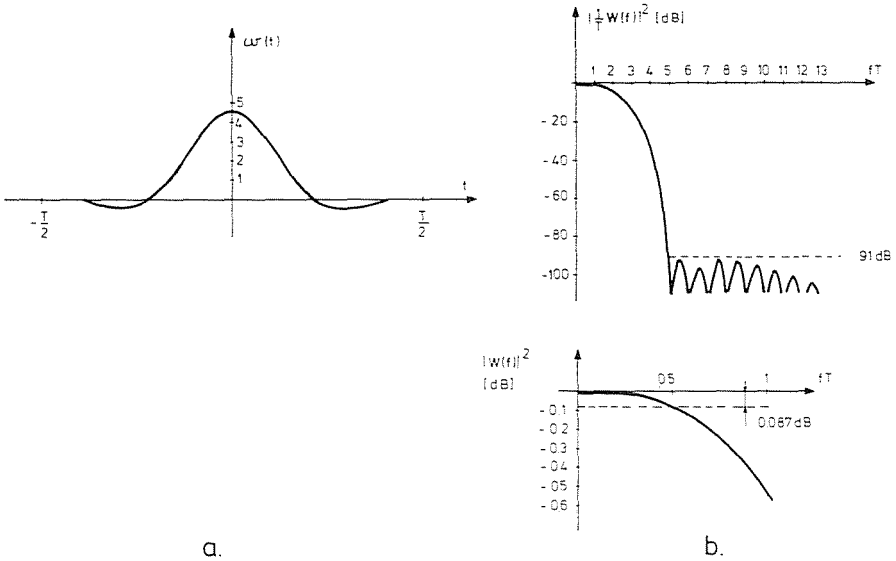
This window is normalized, so that the peak power gain is 1:

$$\left| \frac{1}{T} W(0) \right|^2 = C_0^2 = 1.$$

#### *Variance versus overlap*

After having defined Welch's spectral estimator in (11), now its variance will be examined as a function of the overlap  $\Delta\tau$ . Welch [6] suggests an expression for the covariance between two modified periodograms belonging to different segments:

$$\text{Cov} \{I_x(f, t_1), I_x(f, t_2)\} \approx C(t_2 - t_1, f) \cdot |S_x(f)|^2 \quad (17)$$



a. The large dynamics, little picket - fence window (Ladlipf)  
 a / The time function  
 b / The log plot of the spectral window

Fig. 10. The large dynamics, little picket fence (LADLIPF) window; a) the time function; b) the log plot of the spectral window

Here

$$C(\tau, f) = \vartheta^2(\tau, f) + \vartheta^2(\tau, 0),$$

and

$$\begin{aligned} \vartheta(\tau, f) &= \frac{1}{T_e} \int_{-\infty}^{\infty} W(f-g) W(f+g) e^{j2\pi g\tau} dg = \\ &= \frac{1}{T_e} e^{j2\pi f\tau} \int_{-\infty}^{\infty} w(\tau-t) w(t) e^{-j4\pi ft} dt. \end{aligned} \tag{18}$$

From (18) two important conclusions can be drawn:

1.  $C(\tau, f)$  has a finite support in  $\tau$  for any  $f$ , because  $w(\tau)$  has a finite support as well:  $\text{supp } C(\tau, f) = [-T, T]$  for any  $f$ ;
2. If  $f$  falls into the suppression range of the window then  $\vartheta^2(\tau, f) < 1$ . This implies that

$$C(\tau, f) \approx \vartheta^2(\tau, 0) \quad \text{if } |f| > B.$$

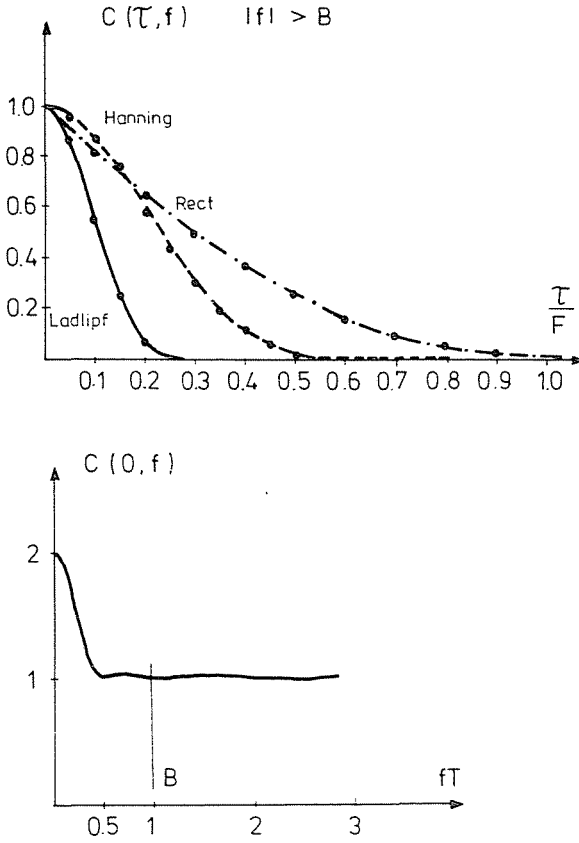


Fig. 11. The  $C(\tau, f)$  function

Applying (17) the variance is arrived at

$$\begin{aligned}
 \text{Var} \{ \hat{S}_x(f) \} &= \frac{1}{K^2} \sum_{i=0}^{K-1} \sum_{k=0}^{K-1} \text{Cov} \{ I_x(f, i\Delta\tau), I_x(f, k\Delta\tau) \} = \\
 &= \frac{S_x^2(f)}{K^2} \sum_{i=0}^{K-1} \sum_{k=0}^{K-1} C[(k-i)\Delta\tau, f] = \\
 &= \frac{S_x^2(f)}{K} \sum_{i=-K}^K C(i\Delta\tau, f) \left( 1 - \frac{|i|}{K} \right). \tag{19}
 \end{aligned}$$

The measuring time  $T_m = T + K\Delta\tau$  is assumed to last much longer than the duration of one segment  $T$ .

Then

$$\begin{aligned} \text{Var} \{ \hat{S}_x(f) \} &\approx \frac{S_x^2(f)}{K} \sum_{i=-K}^K C(i\Delta\tau, f) = \\ &= \frac{S_x^2(f)}{T_m - T} \sum_i C(i\Delta\tau, f) \Delta\tau. \end{aligned} \tag{20}$$

If  $\Delta\tau \rightarrow 0$ , this sum converges to the integral:

$$\lim_{\Delta\tau \rightarrow 0} \text{Var} \{ \hat{S}_x(f) \} = \frac{S_x^2(f)}{T_m - T} \int_{-\infty}^{\infty} C(\tau, f) d\tau. \tag{21}$$

This is the minimal variance possible at a certain measuring time  $T_m$ .

Now, let us introduce the measuring time utilization rate (MTUR), which is a function of  $\Delta\tau$  and  $f$ :

$$\eta(\Delta\tau, f) \triangleq \frac{\lim_{\Delta\tau \rightarrow 0} \text{Var} \{ \hat{S}_x(f) \}}{\text{Var} \{ S_x(f) \}} \approx \frac{\int_{-\infty}^{\infty} C(u, f) du}{\sum_i C(i\Delta\tau, f) \Delta\tau}. \tag{22}$$

There are some MTUR plots versus  $\Delta\tau$  for different windows in Fig. 12. These functions give the overlapping rate necessary for some windows. With decreasing  $\Delta\tau$  (increasing overlap)  $\eta$  converges to 1, but the necessary

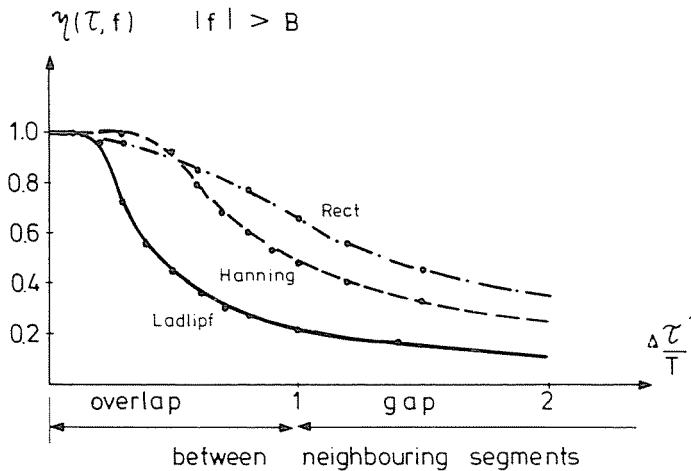


Fig. 12. Some measuring time utilization functions

computation time increases. When  $\Delta\tau$  increases, the correlation between the neighbouring segments decreases, and so does  $\eta(\Delta\tau, f)$  as well. It is obvious from Fig. 11 that when  $C(\tau, f)$  becomes approximately zero, the characteristic of  $\eta(\Delta\tau, f)$  changes: it converges to a hyperbola. So for every window there is a compromise between measuring time utilization and data processing time.

This compromise is about  $\Delta\tau/T=0.5$  for Hanning window, and  $\Delta\tau/T=0.25$  for that suggested above (Fig. 12). In the case  $\Delta\tau/T=1$  there is neither overlap nor gap between the neighbouring segments. Using LADLIPF window in this case, only 22% of the measured information is utilized.

With 75% overlap ( $\Delta\tau/T=0.25$ ) this rate increases to 88%, so assuming the same variance it needs only 1/4 of the measuring time. This problem has a great importance when analyzing random signals with high selectivity and little variance, because such an analysis requires a pretty long measuring time.

### Summary

Frequency analysis is common method for investigating physical phenomena or their signals. Many instruments based on FFT processors have been recently constructed to measure spectra. This paper is concerned with problems of the design and use of such tools and of developing some useful design formulas.

After defining energy spectra, the importance of the Direct Fourier Transform (DRFT) method is pointed out and its error sources outlined. Some DRFT errors such as the variance due to input quantization, the picket fence effect and the variance of the DRFT spectral estimator, and their reduction is dealt with in detail.

### References

1. BENDAT, J. S.—PIERSOL, A. G.: *Random Data: Analysis and Measurement Processes*. John Wiley & Sons, Inc. 1971, New York.
2. SZTIPÁNOVITS, J.: *Optimális mérések kvantált adatokkal (Optimum Measurements with Quantized Data)*. Candidate's Thesis, 1980, Budapest.
3. BRACCINI, C.—OPPENHEIM, A. V.: Unequal Bandwidth Spectral Analysis using Digital Frequency Warping. *IEEE Transactions on Acoustics, Speech and Signal Processing*, Vol. ASSP-22, No. 4, August 1974. pp. 236—244.
4. MCKINNEY, H. W.: Band-Selectable Fourier Analysis. *Hewlett-Packard Journal* Vol. 26. No. 8. April 1975. pp. 20—24.
5. THRANE, N.: Zoom-FFT. *Bruel-Kjaer Technical Review* No. 2. 1980. pp. 3—41.
6. WELCH, P. D.: The Use of Fast Fourier Transform for the Estimation of Power Spectra: A Method Based on Time Averaging over Short, Modified Periodograms. *IEEE Transactions on Audio and Electroacoustics* Vol. AU-15. No. 3. June 1967. pp. 70—73.
7. HARRIS, F. J.: On the Use of Windows for Harmonic Analysis with the Discrete Fourier Transform. *Proceedings of the IEEE*, vol. 66. No. 1. Jan. 1978. pp. 51—83.
8. COX, R. G.: Window Functions for Spectrum Analysis. *Hewlett-Packard Journal*, Vol. 29. No. 13. Sept. 1978. pp. 10—11.
9. NUTTALL, A. H.: Some Windows with Very Good Sidelobe Behavior. *IEEE Transactions on Acoustics, Speech and Signal Processing*, Vol. ASSP-29. No. 1. Febr. 1981. pp. 84—89.

István KOLLÁR      H-1521 Budapest

Ferenc NAGY        Electronic Measuring Gear Works Hungary